Graphene Q-switched Yb:KYW planar waveguide laser

Cite as: AIP Advances 5, 017110 (2015); https://doi.org/10.1063/1.4905785
Submitted: 31 October 2014 • Accepted: 29 December 2014 • Published Online: 08 January 2015

Jun Wan Kim, Sun Young Choi, Shanmugam Aravazhi, et al.

Graphene *Q*-switched Yb:KYW planar waveguide laser

Jun Wan Kim,[1] Sun Young Choi,[1] Shanmugam Aravazhi,[2] Markus Pollnau,[2] Uwe Griebner,[3] Valentin Petrov,[3] Sukang Bae,[4] Kwang Jun Ahn,[1] Dong-Il Yeom,[1,a] and Fabian Rotermund[1,a]

[1]*Department of Energy Systems Research & Department of Physics, Ajou University, 443-749 Suwon, Republic of Korea*

[2]*Integrated Optical Micro Systems Groups, MESA+ Institute of Nanotechnology, University of Twente, 7500 AE Enschede, The Netherlands*

[3]*Max-Born-Institute for Nonlinear Optics and Short Pulse Spectroscopy, 12489 Berlin, Germany*

[4]*Soft Innovative Materials Research Center, Korea Institute of Science and Technology, Jeonbuk 565-905, Republic of Korea*

(Received 31 October 2014; accepted 29 December 2014; published online 8 January 2015)

A diode-pumped Yb:KYW planar waveguide laser, single-mode *Q*-switched by evanescent-field interaction with graphene, is demonstrated for the first time. Few-layer graphene grown by chemical vapor deposition is transferred onto the top of a guiding layer, which initiates stable *Q*-switched operation in a 2.4-cm-long waveguide laser operating near 1027 nm. Average output powers up to 34 mW and pulse durations as short as 349 ns are achieved. The measured output beam profile, clearly exhibiting a single mode, agrees well with the theoretically calculated mode intensity distribution inside the waveguide. As the pump power is increased, the repetition rate and pulse energy increase from 191 to 607 kHz and from 7.4 to 58.6 nJ, respectively, whereas the pulse duration decreases from 2.09 μs to 349 ns. [http://dx.doi.org/10.1063/1.4905785]

Since the first application of graphene as a saturable absorber (SA) in fiber and bulk solid-state lasers, different types of graphene-based SAs have been developed and widely investigated.[1–3] Owing to its unique and outstanding optical properties including ultrabroad absorption, large third-order nonlinearity and ultrafast nonlinear response,[4–6] graphene can initiate pulsed laser operation over a wide spectral range. In particular, relatively simple fabrication processes, the flexible design of devices for direct or indirect interaction with the propagating beam within the laser cavity and the high optical damage threshold originating from the carbon-carbon covalent bonding make graphene SAs alternative *Q*-switching and mode-locking devices[7–10] in addition to widespread semiconductor saturable absorber mirrors (SESAMs).[11]

In recent years, Yb^{3+}-doped crystals possessing upper state lifetimes in the sub-ms range and broad emission bandwidths have proven to be promising gain media for developing efficient continuous wave (cw) and pulsed coherent sources at wavelengths near 1 μm.[11–15] Owing to strong absorption bands around 940, 970, and 980 nm, which are spectrally well-matched to the wavelengths of commercially available low-cost laser diodes, and small quantum defects down to less than 1%[16] in quasi 3-level energy systems reducing the upper state thermal load and quenching process, compact and efficient Yb-doped bulk solid-state lasers have been demonstrated without extra cooling in different cavity configurations.[15–19] To increase the compactness, waveguide lasers based on various waveguiding structures have recently been proposed. The waveguides can be fabricated inside dielectric gain media by various techniques, including diffusion bonding, ion implantation, liquid-phase epitaxy and ultrafast laser inscription.[20–24] Such waveguide geometries additionally

[a]Electronic mail: diyeom@ajou.ac.kr & rotermun@ajou.ac.kr

provide high intra-cavity pump intensity even with low-power pumping, excellent overlap of the pump and cavity modes, and efficient heat dissipation. The operation of waveguide lasers Q-switched or mode-locked using SESAMs and other SAs based on Cr-doped crystals, carbon nanotubes and graphene has been demonstrated.[22–30] In most cases, however, a direct interaction scheme of light with the SAs, i.e., placing the SA perpendicular to the resonator axis, was employed. To reduce the damage susceptibility and thermal load of SAs, indirect interaction by evanescent-field coupling was recently suggested for Q-switching and mode-locking.[8,27,28] In the present work we demonstrate, for the first time, Q-switched operation of an Yb^{3+}:$KY(WO_4)_2$ (Yb:KYW) planar waveguide laser through evanescent field coupling with few-layer graphene deposited on the top surface of the waveguide. The lateral interaction scheme increases the nonlinear interaction length between graphene and the beam propagating within the waveguide. By optimizing the length and position of the deposited graphene, we are able to achieve stable single-mode Q-switched operation with average output powers up to 34 mW at 1027 nm. Additionally, in contrast to the Q-switched Nd:YAG waveguide laser reported in Ref. 28, we are able to observe a transition from stable Q-switching to an intermediate state of mode-locking for the first time in a planar waveguide laser.

For the laser experiments an Yb^{3+} (1.7 at. %) doped KYW planar waveguide is chosen as the gain medium. The fabrication procedure is described in detail in Ref. 20. The Yb:KYW guiding layer with a thickness of 26.4 μm is grown onto the polished (010) surface of an undoped KYW substrate by liquid phase epitaxy. The fabricated Yb:KYW/KYW planar waveguide is subsequently cut to a length of 6 mm along the N_g-dielectric axis, and both end faces are polished to a high optical quality. To realize Q-switched operation by evanescent-field interaction with the SA, few-layer graphene is transferred onto the top of the Yb:KYW guiding layer. The few-layer graphene used as the SA is first grown onto a copper foil by chemical vapor deposition (CVD); a similar procedure is described elsewhere.[31] An as-grown few-layer graphene coated with poly (methyl methacrylate) (PMMA) as supporting layer, to enhance efficient evanescent-field coupling, is then transferred onto the top of the Yb:KYW planar waveguide after removal of the copper foil by etching. One half of the whole top area of the waveguide, i.e., ~3 mm of the propagation length, is covered with the graphene, whose linear absorption is measured as 7.8% around the laser operation wavelength.

The laser oscillator comprises the Yb:KYW planar waveguide, an achromatic lens, and two mirrors including a 4% output coupler (OC), as shown in Fig. 1. A polarization-maintaining fiber-coupled single-mode laser diode (LD) operating at 980 nm (CHP1999, 3S photonics) serves as the pump source, and a Faraday isolator (IO-5-980-HP, Thorlabs) is inserted between the LD and a half-wave plate to prevent back reflection of the pump beam to the LD. The half-wave plate ensures that the pump beam polarization is parallel to the N_m axis of the Yb:KYW waveguide. The collimated pump beam is then focused into the planar waveguide by a lens through the dichroic plane mirror serving as input coupler. The focused beam diameter at the position of the waveguide endface is estimated using the knife-edge method as 23.6 μm, which is slightly smaller than the

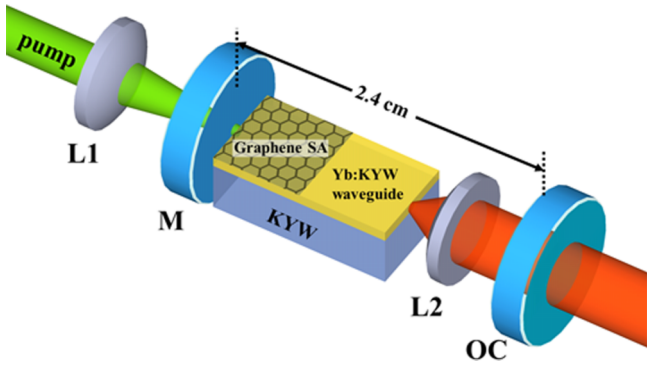

FIG. 1. Schematic of the Yb:KYW planar waveguide laser Q-switched by evanescent-field interaction with graphene. L1, convex lens with a focal length of f = 50 mm; L2, aspheric lens with f = 6.24 mm; M, dielectric plane mirror (high transmission at 980 nm and broadband high reflection near 1030 nm); OC, 4% output coupler.

thickness of the waveguide. An aspheric lens is inserted between the waveguide and OC to maintain efficient mode matching both in the vertical and horizontal planes within the waveguide and to increase the stability range of the resonator. The laser output beam is finally collimated using a convex lens for further characterization.

Before investigating the performance of the Yb:KYW planar waveguide laser *Q*-switched by the evanescent-field coupling with the deposited graphene SA, the cw operation is characterized. CW lasing starts at an incident pump power of 221 mW and a maximum output power of 93 mW at 1028 nm is achieved with 724-mW pumping. The slope efficiency amounts to 20.2% in the cw regime with respect to the incident pump power. At a given pump power *Q*-switching does not occur automatically when the laser cavity is optimized for maximum cw output power. *Q*-switched operation of the Yb:KYW planar waveguide laser is obtained by careful alignment of the cavity length and the position of the intra-cavity lens. The *Q*-switching is stable when the cavity length is adjusted to 2.4 cm. The measured laser spectrum in this regime, centered at 1027 nm with a spectral bandwidth of 1.7 nm, is shown in Fig. 2. The *Q*-switched pulse train is recorded by a fast photodiode (InGaAs PIN detector ET-3500, EOT, 15 GHz, 25 ps) and an oscilloscope (TDS 7254, Tektronix, 2.5 GHz, 20 Gs/s) (inset of Fig. 2). The repetition rate varies from 191 kHz to 607 kHz as the pump power increases, as is shown in the upper row of Fig. 3(a). This behavior is typical for passively *Q*-switched lasers and occurs, because the repetition rate is proportional to the peak intensity in the laser cavity and strongly depends on the transition rate of the gain and the saturation level of the absorber.[32,33] The pulse duration of the *Q*-switched laser pulses is also measured for different pump powers. The lower row of Fig. 3(a) shows a decrease in the pulse duration from 2.09 μs to 349 ns when the pump power increases. The corresponding single-pulse energy, which increases from 7.4 to 58.6 nJ, is depicted in the upper row of Fig. 3(b). The lower row of Fig. 3(b) displays the measured input-output power characteristics. The *Q*-switching pump threshold is measured as 324 mW, and *Q*-switching is easily achieved above this threshold up to the maximum output power of 34 mW, corresponding to the single-pulse energy of 58.6 nJ. The slope efficiency in this case is 9.1%.

The spatial beam profile in the stable *Q*-switched regime indicates almost a single transverse mode, whereas the beam profile in cw operation shows either a distorted single or double mode in the vertical direction when the output power is aligned to the maximum. The reduced slope efficiency in *Q*-switched operation in comparison with the cw case is attributed mainly to the different mode profiles in the slightly different cavities and the different evanescent-field coupling strengths with the SA, which lead to different linear and nonlinear losses in the cavity.

The measured spatial beam profile of the laser output is compared with the calculated mode intensity distribution inside the planar waveguide. Figure 4(a) shows the structure of the waveguide

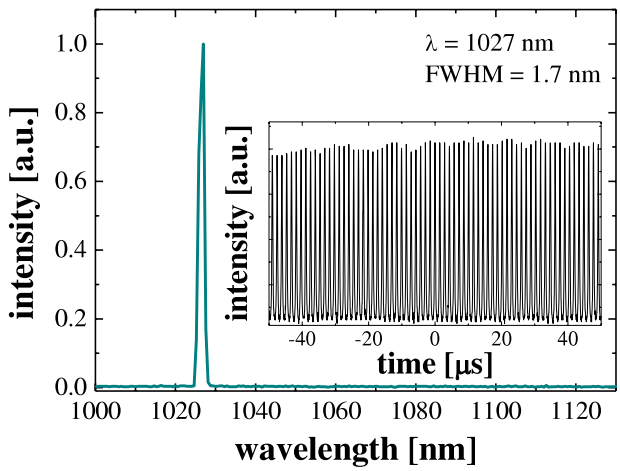

FIG. 2. Graphene *Q*-switched Yb:KYW planar waveguide laser by evanescent-field interaction: optical spectrum and pulse train (inset).

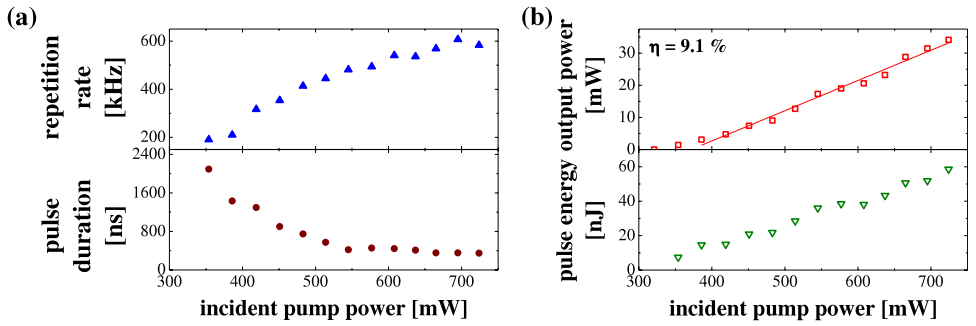

FIG. 3. Graphene Q-switched Yb:KYW planar waveguide laser by evanescent-field interaction: (a) dependence of repetition rate (upper) and pulse duration (lower) on input pump power and (b) pulse energy (upper) and average output power with linear fit (lower).

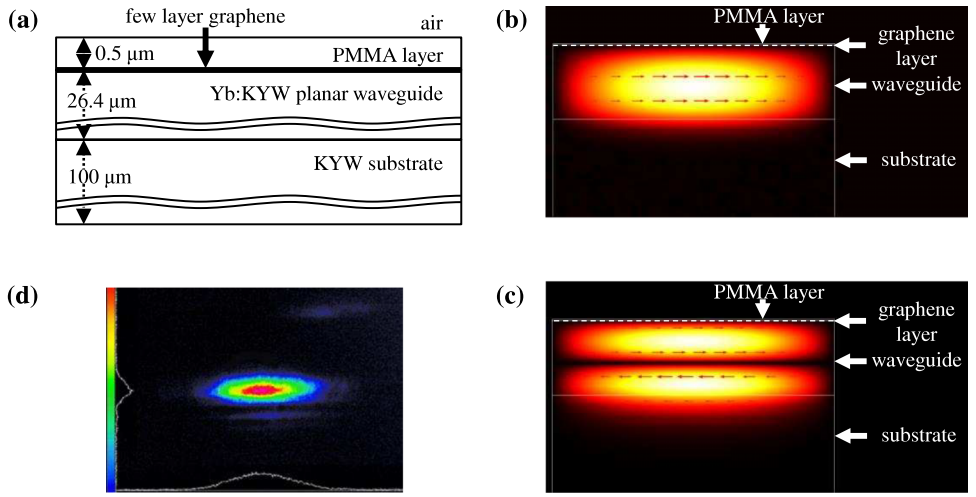

FIG. 4. (a) Structure of the grapnene depositied Yb:KYW planar waveguide, calculated propagating beam profiles of (b) the fundamental (TE_0) and (c) the second-order (TE_1) guided modes and (d) measured beam profile in Q-switched operation.

used in this work. The refractive indices of the PMMA layer, few-layer graphene, Yb:KYW guiding layer and KYW substrate are assumed as 1.4817, 3, 2.0006, and 2, respectively,[21,34] and their thicknesses are set to 0.5 μm, 1.02 nm, 26.4 μm, and 100 μm, respectively, as illustrated in Fig. 4(a). As expected, our planar waveguide supports multiple spatial modes in the vertical direction owing to the relatively thick guiding layer. Figures 4(b) and 4(c) show the calculated beam profiles of the fundamental and second-order transverse-electric (TE) guided modes. The ultrathin graphene layer has only negligible influence on the mode calculation. The fundamental mode in Fig. 4(b) is tightly confined inside the waveguide, whereas the first higher-order mode in Fig. 4(c) extends further into the substrate. In the *Q*-switching experiment, we adjust the position of the intra-cavity lens and the cavity length to achieve the clear fundamental mode by efficient beam coupling while monitoring the spatial beam profile. Although *Q*-switched pulses can be generated also in multi-mode operation, this regime is unstable and can be sustained only for a limited time. Figure 4(d) presents the image of the intensity distribution of the single-transverse-mode Q-switched laser, measured after the OC, with the horizontal and vertical intensity profiles. The output beam is almost single mode, as expected from the theoretical calculation. The low-intensity ripples appearing in the vertical direction below the fundamental mode are mainly attributed to artifacts created by the undesired interference of the reflected beam in the Fabry-Perot-type resonator.

When the cavity length is reduced to 2.25 cm and the position of the intra-cavity lens and OC are carefully realigned, we observe a transition from stable *Q*-switching to an intermediate state with mode-locking. Figure 5 shows the measured pulse train in this intermediate regime, depicted

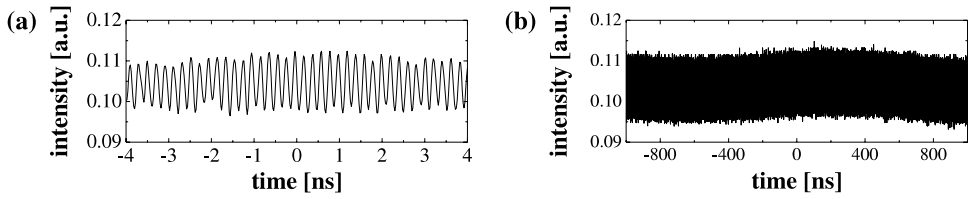

FIG. 5. Oscilloscope trace of the mode-locked signal on *Q*-switched envelope in different spans of (a) 2 μs and (b) 8 ns.

in two different spans. The unstable modulation of the mode-locked pulses can be observed on the *Q*-switched envelope. The separation between the modulated signals corresponds to the repetition rate of 4.81 GHz, which agrees well with the effective cavity length of our planar waveguide laser. The number of logitudinal modes in the measured optical spectrum is caclulated to be 278. A direct measurement of the pulse duration by auto-correlation cannot be performed at this stage, because the pulse energy of < 7 pJ estimated for the given repetition rate is too low. To realize stable passive mode-locking of the planar waveguide by the evanescent-field coupling, a new waveguide sample of reduced thickness will be needed and the interaction with the graphene SA shall also be further optimized.

In summary, we report the laser performance of a graphene *Q*-switched Yb:KYW planar waveguide laser by evanescent-field interaction. The CVD-grown few-layer graphene SA deposited on top of the Yb:KYW guiding layer provides efficient saturable absorption by evanescent-field coupling between the guided fundamental mode and graphene. The *Q*-switched Yb:KYW planar waveguide laser delivers 349-nJ pulses with a maximum output power of 34 mW, corresponding to a single-pulse energy of 58.6 nJ at a 607-kHz repetition rate. The pulse duration and repetition rate can be tuned from 2.09 μs to 349 ns and from 191 to 607 kHz, respectively. The spatial intensity distribution of the laser beam indicates stable *Q*-switched single-mode operation. A transition from *Q*-switching to mode-locking enabling generation of much shorter pulses is also observed for the first time in a planar waveguide laser by adjustment of the resonator length and fine alignments. We believe that our concept, i.e., the SA-integrated waveguide as a gain medium in a geometry employing evanescent-field interaction, can be further improved to demonstrate not only compact *Q*-switched, but also mode-locked waveguide lasers.

ACKNOWLEDGMENTS

This work has been supported by the National Research Foundation (NRF) grants funded by Korea Government (MEST and MSIP) (2011-0017494, WCI 2011-001, 2008-0061906 and CAMM 2014M3A6B3063709). This work was also partly supported by the ICT R&D program of MSIP/ IITP. (100325602, Core Technology Development of Laser Accelerated Ion-Beam Generation System). S. Bae appreciate the financial support from the Korea Institute of Science and Technology (KIST) Institutional Program.

[1] Z. Sun, T. Hasan, F. Torrisi, D. Popa, G. Privitera, F. Wang, F. Bonaccorso, D. M. Basko, and A. C. Ferrari, ACS Nano **4**, 803 (2010).
[2] F. Bonaccorso, Z. Sun, T. Hasan, and A. C. Ferrari, Nat. Photonics **4**, 611 (2010).
[3] Q. Bao, H. Zhang, Y. Wang, Z. Ni, Y. Yan, Z. X. Shen, K. P. Loh, and D. Y. Tang, Adv. Funct. Mater. **19**, 3077 (2009).
[4] A. K. Geim and K. S. Novoselov, Nat. Mater. **6**, 183 (2007).
[5] E. Hendry, P. J. Hale, J. Moger, and A. K. Savchenko, Phys. Rev. Lett. **105**, 097401 (2010).
[6] H. Wang, J. H. Strait, P. A. George, S. Shivaraman, V. B. Shields, M. Chandrashekhar, J. Hwang, F. Rana, M. G. Spencer, C. S. Ruiz-Vargas, and J. Park, Appl. Phys. Lett. **96**, 081917 (2010).
[7] D. Popa, Z. Sun, T. Hasan, F. Torrisi, F. Wang, and A. C. Ferrari, Appl. Phys. Lett. **98**, 073106 (2011).
[8] S. Y. Choi, H. Jeong, B. H. Hong, F. Rotermund, and D.-I. Yeom, Laser Phys. Lett. **11**, 015101 (2014).
[9] H. Zhang, D. Y. Tang, L. M. Zhao, Q. L. Bao, and K. P. Loh, Opt. Express **17**, 17630 (2009).
[10] W. B. Cho, J. W. Kim, H. W. Lee, S. Bae, B. H. Hong, S. Y. Choi, I. H. Baek, K. Kim, D.-I. Yeom, and F. Rotermund, Opt. Lett. **36**, 4089 (2011).
[11] C. Hönninger, F. Morier-Genoud, M. Moser, U. Keller, L. R. Brovelli, and C. Harder, Opt. Lett. **23**, 126 (1998).
[12] P. Lacovara, H. K. Choi, C. A. Wang, R. L. Aggarwal, and T. Y. Fan, Opt. Lett. **16**, 1089 (1991).
[13] N. V. Kuleshov, A. A. Lagatsky, A. V. Podlipensky, and V. P. Mikhailov, Opt. Lett. **22**, 1317 (1997).

[14] M. Pollnau, Y. E. Romanyuk, F. Gardillou, C. N. Borca, U. Griebner, S. Rivier, and V. Petrov, IEEE J. Sel. Top. Quant. **13**, 661 (2007).
[15] A. Major, D. Sandkuijl, and V. Barzda, Opt. Express **17**, 12039 (2009).
[16] D. Geskus, S. Aravazhi, K. Wörhoff, and M. Pollnau, Opt. Express **18**, 26107 (2010).
[17] S. Pekarek, C. Fiebig, M. C. Stumpf, A. E. H. Oehler, K. Paschke, G. Erbert, T. Südmeyer, and U. Keller, Opt. Express **18**, 16320 (2010).
[18] H.-W. Yang, C. Kim, S. Y. Choi, G.-H. Kim, Y. Kobayashi, F. Rotermund, and J. Kim, Opt. Express **20**, 29518 (2012).
[19] S. Y. Choi, J. W. Kim, M. H. Kim, D.-I. Yeom, B. H. Hong, X. Mateos, M. Aguiló, F. Diaz, V. Petrov, U. Griebner, and F. Rotermund, Opt. Express **22**, 15626 (2014).
[20] R. J. Beach, S. C. Mitchell, H. E. Meissner, O. R. Meissner, W. F. Krupke, J. M. McMahon, W. J. Bennett, and D. P. Shepherd, Opt. Lett. **26**, 881 (2001).
[21] Y. E. Romanyuk, C. N. Borca, M. Pollnau, S. Rivier, V. Petrov, and U. Griebner, Opt. Lett. **31**, 53 (2006).
[22] Y. Tan, S. Akhmadaliev, S. Zhou, S. Sun, and F. Chen, Opt. Express **22**, 3572 (2014).
[23] Y. Tan, Q. Luan, F. Liu, F. Chen, and J. R. V. Aldana, Opt. Express **21**, 18963 (2013).
[24] T. Calmano, A. G. Paschke, J. Siebenmorgen, S. T. Fredrich-Thornton, H. Yagi, K. Petermann, and G. Huber, Appl. Phys. B **103**, 1 (2011).
[25] A. Choudhary, A. A. Lagatsky, P. Kannan, W. Sibbett, C. T. A. Brown, and D. P. Shepherd, Opt. lett. **21**, 4416 (2012).
[26] J. I. Mackenzie and D. P. Shepherd, Opt. Lett. **27**, 2161 (2002).
[27] J. W. Kim, S. Y. Choi, D.-I. Yeom, S. Aravazhi, M. Pollnau, U. Griebner, V. Petrov, and F. Rotermund, Opt. Lett. **38**, 5090 (2013).
[28] Y. Tan, C. Cheng, S. Akhmadaliev, S. Zhou, and F. Chen, Opt. Express **22**, 9101 (2014).
[29] R. Mary, G. Brown, S. J. Beecher, F. Torrisi, S. Milana, D. Popa, T. Hasan, Z. Sun, E. Lidorikis, S. Ohara, A. C. Ferrari, and A. K. Kar, Opt. Express **21**, 7943 (2013).
[30] A. Choudhary, S. Dhingra, B. D'Urso, T. L. Parsonage, K. A. Sloyan, R. W. Eason, and D. P. Shepherd, Opt. Lett. **39**, 4325 (2014).
[31] S. Bae, H. Kim, Y. Lee, X. Xu, J.-S. Park, Y. Zheng, J. Balakrishnan, T. Lei, H. R. Kim, Y. I. Song, Y.-J. Kim, K. S. Kim, B. Özyilmaz, J.-H. Ahn, B. H. Hong, and S. Iijima, Nat. Nanotechnol. **5**, 574 (2010).
[32] J. A. Morris and C. R. Pollock, Opt. Lett. **15**, 440 (1990).
[33] X. Zhang, S. Zhao, Q. Wang, Q. Zhang, L. Sun, and S. Zhang, IEEE J. Quantum Electron. **33**, 2286 (1997).
[34] J. W. Weber, V. E. Calado, and M. C. M. van de Sanden, Appl. Phys. Lett. **97**, 091904 (2010).